Casimir forces of metallic microstructures into cavities

George Kenanakis,[1,*] Costas M. Soukoulis,[1,2] and Eleftherios N. Economou[1]
[1]*Institute of Electronic Structure and Laser, Foundation for Research and Technology–Hellas, N. Plastira 100, 70013 Heraklion, Crete, Greece*
[2]*Ames Laboratory–USDOE, and Department of Physics and Astronomy, Iowa State University, Ames, Iowa 50011, USA*
(Received 7 June 2015; revised manuscript received 31 July 2015; published 19 August 2015)

A theoretical estimate of the Casimir force of a metallic structure embedded into a cubic cavity is proposed. We demonstrate that by calculating the eigenmodes of the system we can determine the Casimir force, which can be either attractive or repulsive, by simply changing the geometry of the structures relative to the walls of the cavity. In this analysis, several cases of structures are taken into account, from rectangular slabs to chiral "omega" particles, and the predicted data are consistent with recent literature. We demonstrate that the sidewalls of the studied cavity contribute decisively to the repulsive Casimir force between the system and the nearby top surface of the cavity. Finally, we provide evidence that the medium embedded into the studied cavity (and especially its permittivity) can change the intensity of the Casimir force, while its repulsive nature, once established (owing to favorable geometrical features), remains quite robust.

DOI: 10.1103/PhysRevB.92.075430 PACS number(s): 42.50.Ct, 12.20.−m, 78.20.Ek, 81.05.Xj

I. INTRODUCTION

The Casimir force has been widely studied over the past years [1–4], giving emphasis to its practical applications [5,6]. According to Casimir, who discovered this force [7], two neutral, perfectly conducting parallel surfaces in vacuum separated by a distance d attract each other by a force F due to the quantum fluctuations of the vacuum field [7,8], $(F/A) = -\frac{\pi^2}{240}\frac{\hbar c}{d^4}$, where $\hbar$ is the Planck constant divided by 2π, and A is the area. The Casimir force becomes more pronounced if the dimension goes to nanoscale, leading to stiction and adhesion on the surface [2], which is a challenge for flexibly operating the microelectromechanical and nanoelectromechanical system devices (MEMs and NEMs).

Lifshitz's extended theory [9] generalized the calculation of the Casimir force between two parallel plates, 1 and 2, characterized by frequency-dependent dielectric functions $\varepsilon_1(\omega)$ and $\varepsilon_2(\omega)$. The formula for the force or the interaction energy per unit area can be expressed in terms of the reflection amplitudes r_j^{ab} $(j = 1, 2)$ [10] at the interface between the vacuum and the plate j, giving the ratio of the reflected electromagnetic wave of polarization a over the incoming wave of polarization b. Each a and b stands for either transverse magnetic (TM, or p) or transverse electric (TE, or s) polarized waves. The frequency integration is μ_0 performed along the imaginary axis by setting $\omega = i\xi$. The interaction energy per unit area is given by

$$\frac{E(d)}{A} = \frac{\hbar}{2\pi}\int_0^{+\infty} d\xi \int \frac{d^2k_{||}}{(2\pi)^2} \ln\det G, \quad R_j = \begin{vmatrix} r_j^{ss} & r_j^{sp} \\ r_j^{ps} & r_j^{pp} \end{vmatrix}, \tag{1}$$

where $G = I - R_1 \cdot R_2 e^{-2K_0 d}$, I is the unit matrix, and $K_0 = \sqrt{k_{||}^2 + \varepsilon_0\mu_0\xi^2}$; ε_0 and μ_0 are the permittivity and permeability of free space, and d is the distance between the two parallel plates. A negative slope of $E(d)$ corresponds to a repulsive force, while a positive one corresponds to an attractive force.

The calculation of the Casimir force was extended to other than planar geometries [1,11,12], because a unique property of this force is its strong dependence on the geometry of the interacting media, switching from attractive to repulsive; this makes the Casimir effect a likely candidate for applications in nanotechnologies and MEMs [13]. The attractive Casimir forces are predicted to exist between electrically neutral bodies [13], while repulsive forces are predicted to exist inside of an empty sphere [1] and an empty rectangular cavity [11,12] with perfectly conducting walls.

In this paper we study numerically the effect of the geometry of a metallic structure inside a metallic cavity on the attractive or repulsive character of the Casimir force. More explicitly, we introduce several metallic structures of various sizes and shapes inside a $3 \times 3 \times 3\,\mu\text{m}^3$ metallic cavity and close to the top surface; then, the basic approach employed is the calculation of the eigenmodes of the system, in whose terms we determine the Casimir interaction and hence the force, which can be either attractive or repulsive, by simply changing the geometrical features of the structures.

II. STRUCTURES UNDER INVESTIGATION

The structures employed in the present study, shown in Figs. 1(a)–1(d), were placed inside a $3 \times 3 \times 3\,\mu\text{m}^3$ metallic cavity, close to its top surface [see Fig. 1(a)]; their geometrical parameters are detailed in the caption of Fig. 1.

As one can see in Fig. 1, apart from the square structures of Fig. 1(a) with $L = 0.055$–$1.375\,\mu$m, three more structures embedded in metal cavities were studied [see Figs. 1(b)–1(d) for details]: a metallic ring of circular cross section with diameter $H = 0.150\,\mu$m and outer diameter of $w = 2.75\,\mu$m [Fig. 1(b)], a split ring resonator (SRR)-like structure (loop) having the same geometrical dimensions as the ring in Fig. 1(b) and a gap of $H = 0.150\,\mu$m [Fig. 1(c)], and a chiral "omega" structure consisting of an open circular loop with exactly the same dimensions as the SRR structure of Fig. 1(c) and two short wires with a length $a = 1.0\,\mu$m, as seen in Fig. 1(d).

*gkenanak@iesl.forth.gr

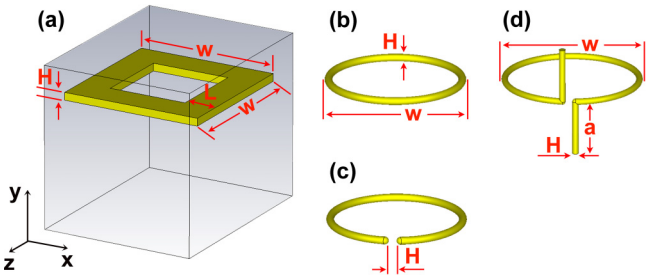

FIG. 1. (Color online) Schematic of the structures under investigation; $w = 2.75\,\mu$m, $H = 0.15\,\mu$m, $L = 0.055$–$1.375\,\mu$m, and $a = 0$–$1.125\,\mu$m, respectively. In (a) one can notice the $3 \times 3 \times 3\,\mu\text{m}^3$ metallic cavity, in which each of the studied structures are embedded, close to its top surface.

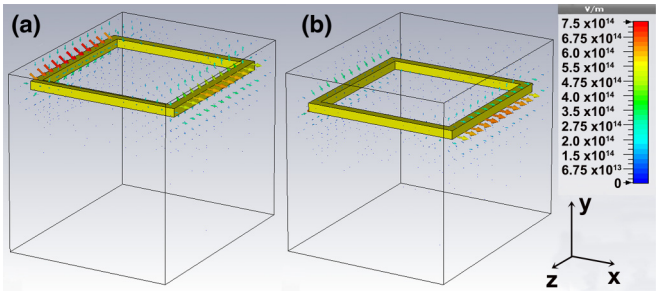

FIG. 2. (Color online) The $3 \times 3 \times 3\,\mu\text{m}^3$ boundary box acting as a metallic cavity with the metallic structure (with $L = 0.150\,\mu$m) embedded into it. The distance of the structure from the top surface of the boundary box is (a) 100 and (b) 500 nm, respectively. A snapshot of the electric field distribution on the metallic structure embedded into the $3 \times 3 \times 3\,\mu\text{m}^3$ boundary box is shown.

III. NUMERICAL SIMULATIONS: ESTIMATION OF THE CASIMIR FORCE

For the numerical simulations we used the eigenmode solver of a commercial three-dimensional full-wave solver (CST Microwave Studio, Computer Simulation Technology GmbH, Darmstadt, Germany) based on the finite integration technique. For each design we considered a single ($3 \times 3 \times 3\,\mu\text{m}^3$) calculation boundary box under vacuum, as shown in Fig. 1(a), with the tangential electric field being zero ($E_t = 0$) along the x, y, and z directions, acting as a perfectly metallic cavity, while all the metallic structures (yellow color in Fig. 1) were treated as perfect electric conductors (PECs), since the eigenmode solver of the software mentioned above does not support lossy and/or dispersive metal materials.

At this point it should be noted that Casimir force arises from the fluctuations of the electromagnetic field mainly in the region between the metallic surface (a), and from a van der Waals type of interaction due to electrostatic mutual polarization of the metallic materials (b). The (a) part can equivalently be incorporated into (b) by including retardation effects [14]. The first contribution dominates at distances much larger than a characteristic absorption length $\lambda_0 \equiv c/\omega_0$ [14], where ω_0 is a frequency corresponding to a characteristic excitation energy $\hbar\omega_0$ in a metal, such as a plasma energy. The length λ_0 physically is the one beyond which the usual electrostatic van der Waals interaction has to be corrected as to incorporate retardation effects [14]. The second contribution to the Casimir force, mentioned above, prevails at much smaller distances [14], typically for λ_0 in the order of 30 nm [15]. As a result, our calculations, although we consider PEC structures and not a realistic frequency-dependent permittivity of the metallic structures and the walls of the cavity, are safe.

Moreover, as in our case, there are several research groups [16,17] calculating the Casimir force considering PEC structures in metallic cavities with PEC walls filled with nondispersive media, indicating that the effect of loss and dispersion is quite mild and that the results obtained using the PEC assumption describe well the physics of the system.

The structures under investigation were placed into the cavity described above, initially at a distance d of 100 nm from its top surface [see Fig. 2 for the case of the structure presented in Fig. 1(a) with $L = 150$ nm]. Using the eigenmode solver of the CST software, the first 500 eigenmodes of the system (PEC structure into the cavity) were calculated. The energy of the system was calculated using the formula [13]

$$E_d = \frac{1}{2}\sum_{i=1}^{500} \hbar\omega_i, \tag{2}$$

where d denotes the distance between the center of the studied structure and the top surface of the cavity, and ω_i denotes each of the 500 calculated eigenmodes. Then, each of the PEC structures was moved along the y axis at a distance of 200 and 500 nm from the top surface of the boundary box, respectively [see Fig. 1(a)], and the corresponding energies $E_{200\,\text{nm}}$ and $E_{500\,\text{nm}}$ were calculated.

In order to estimate the Casimir force (F) along the y axis at a distance $d = 300$ nm between the top surface of the cavity and the PEC structure, the following formula was used:

$$F_{y,300\,\text{nm}} = \frac{E_{d=500\,\text{nm}} - E_{d=100\,\text{nm}}}{500\text{–}100\,\text{nm}} \approx \frac{E_{d=200\,\text{nm}} - E_{d=100\,\text{nm}}}{200\text{–}100\,\text{nm}}, \tag{3}$$

where $E_{d=500\,\text{nm}}$, $E_{d=200\,\text{nm}}$, and $E_{d=100\,\text{nm}}$ are the calculated energies at distances of 500, 200, and 100 nm, respectively.

As one can notice from Fig. 2, the contribution of the sidewalls of the metallic cavity is more intense than the one from the top (and of course the bottom) walls. Following the methodology described above, we have calculated the Casimir force of the structures presented in Fig. 1(a) for several values of L, keeping H constant and equal to 150 nm. We have repeated these calculations for $H = 50$ nm and for $H = 300$ nm, changing the geometry of Fig. 1(a) from a rectangular loop with $L = 0.055\,\mu$m ($L/H = 0.367$) to a square plate with $L = 1.375\,\mu$m ($L/H = 9.167$). In Fig. 3 we present the Casimir force of the proposed structure of Fig. 1(a) along the y axis, as a function of the ratio L/H.

As seen from Fig. 3, there is a certain value of the ratio $L/H = 1.167$ where the Casimir force along the y axis (at a distance of about $d \approx 225$ nm between the top surface of the cavity and the PEC structure) is equal to zero. Moreover, for $1.167 < L/H \leqslant 9.167$, a negative Casimir force is obtained, indicating that the force is attractive, while for, a positive Casimir force is achieved, demonstrating that the force is repulsive.

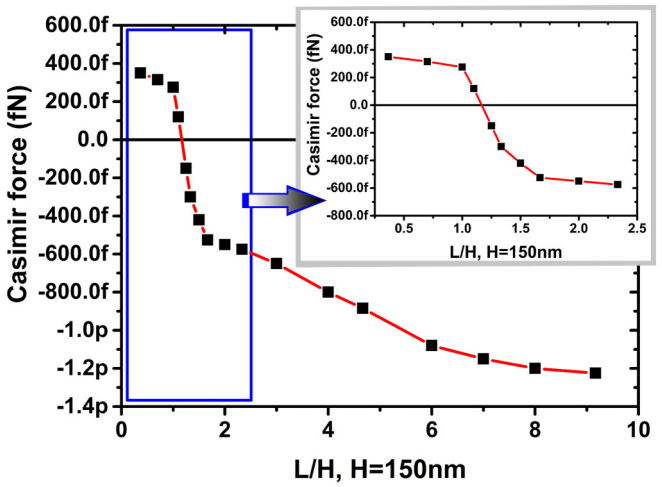

FIG. 3. (Color online) Casimir force along the y axis at a distance $d = 300$ nm between the top surface of the cavity and the proposed structure of Fig. 1(a) as a function of the ratio L/H. In the inset, one can see a more detailed presentation of the Casimir force for $L/H = 0.25$–2.5.

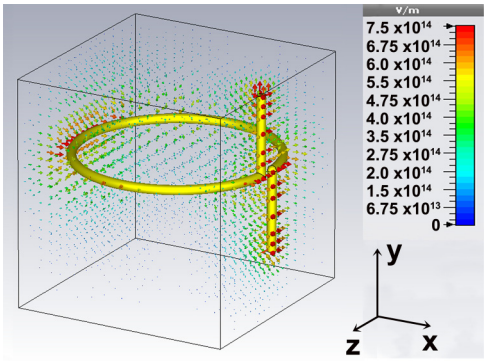

FIG. 4. (Color online) Electric field distribution on the "omega" particle embedded into the $3 \times 3 \times 3\,\mu m^3$ cavity at a distance of 100 nm between the upper edge of the wire and the top surface.

At this point it is worth mentioning again that further numerical simulations have been performed (not shown here) for values of H other than 150 nm, and 300 nm, respectively, and by changing the values of L. As in the case of and $L = 0.055$–$1.375\ \mu$m ($L/H = 0.367$–9.167), we found again using these other values of H that there is a region for L/H in which a negative (attractive) Casimir force is obtained, while for a different region of L/H a positive (repulsive) Casimir force is achieved and that the transition occurs for the same value of the ratio L/H. Thus, it was concluded that it is the ratio L/H which controls the sign of the Casimir force between the object and the top wall in the presence of sidewalls. This behavior is attributed to a competition between the interaction with the sidewalls, which is producing a repulsive force along the y direction, and the interaction with the top wall, which produces an attractive force along the same direction. (The bottom wall is too far away to play any role). Obviously, as L is increasing, the interaction with the top is enhanced and overcomes the repulsion. On the other hand, as the length H is increasing, the repulsion due to the sidewall is strengthened and wins over the attraction. Thus, it is the ratio L/H which controls the sign of the Casimir force between the object and the top wall in the presence of sidewalls. We think, on the basis of our results and those of Ambjørn and Wolfram [12], that in general the presence of a kind of surrounding side metal contributes a repulsive component to the Casimir force.

Let us summarize the preceding arguments: Our assertion that the sidewalls contribute a repulsive component to the force along the y direction, while the top wall contributes an attractive one, is supported both by the obtained field distributions (Figs. 2 and 4) and the simulations showing that (attractive component)/(repulsive component) is a monotonically decreasing function of the ratio L/H.

According to Zhao *et al.* [18], the intensity of the repulsive Casimir force can be optimized by increasing the inductance of the structures. Indeed, the rectangular and the circular metallic rings of Fig. 1(a) with $L/H = 1$ and Fig. 1(b), respectively, give almost the same repulsive Casimir forces, 275 and 273.7 fN, respectively. When a gap is created in the metallic ring structure [see Fig. 1(c)] (and thus inductance is induced), the Casimir force remains repulsive, while its intensity is raised to 283.5 fN.

Another important parameter for enhancing the repulsive Casimir force is the chiral properties of the structures [18,19]. As already stated [15,18], chiral metamaterials (CMMs) are candidates to realize the repulsive Casimir force, while the existence of a repulsive Casimir force depends upon the strength of the chirality. Indeed, the so-called "omega" particle [18,20], defined in Fig. 1(d), provided a repulsive Casimir force along the y axis with an intensity of $\sim$315.1 fN, enhanced by $\sim$11.2% compared to the SRR structure presented in Fig. 1(c), exhibiting the highest repulsive Casimir force compared to all the structures studied in this work (see Fig. 1 for reference).

Moreover, as already stated for the structures shown in Fig. 2, the contribution of the sidewalls of the metallic cavity is more intense than the one from the top wall (the interaction with the bottom wall is still quite small, even in the case of the omega particle shown in Fig. 4, where the distance between the lower edge and the bottom is 0.75 μm). This is confirmed by the electric field distribution shown in Fig. 4, where the upper edge of the "omega" particle is at a distance of 100 nm from the top surface of the cavity [the distance between the loop of the "omega" structure and the top surface of the cavity is equal to 1.1 μm (0.1 μm + a), and the distance of the lower edge from the bottom surface is 0.75 μm (3–2a–0.15 μm–0.1 μm), where a is the length of the "omega's" wires, taken to be equal to 1.0 μm, in Fig. 4].

The omega particle can be considered as a connection of two small wire antennas: a short electric dipole antenna of length $2a$ and a small loop antenna with radius $2.75/2\ \mu$m [21–23]. Since the length (a in Fig. 5) of the wires of the omega particle enhances the chirality the structure, its effect on the Casimir force is further investigated. In Fig. 5 one can see the intensity of the Casimir force along the y axis (in fN) of the proposed omega particle embedded into a $3 \times 3 \times 3\,\mu m^3$ cavity, as a function of its wire's length a. For these types of calculations, the loop of the omega particle was placed at a symmetric

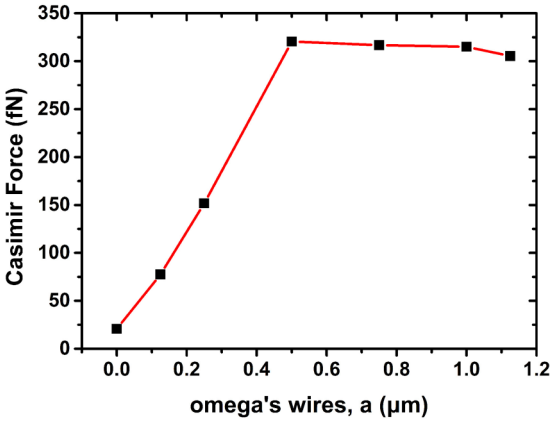

FIG. 5. (Color online) Repulsive Casimir force of the proposed "omega" particle embedded into a $3 \times 3 \times 3\,\mu\text{m}^3$ cavity, as a function of its wire's length a. For these types of calculations, as opposed to the one shown in Fig. 4, the loop of the "omega" particle was placed at a symmetric position in the $3 \times 3 \times 3\,\mu\text{m}^3$ cavity, and several cases of wires were studied with length $a = 0.0$–$1.125\,\mu$m.

position in the $3 \times 3 \times 3\,\mu\text{m}^3$ cavity, and several cases of wires were studied with a length $a = 0.0$–$1.125\,\mu$m. Then, the omega particle was moved towards the top surface of the cavity by 100 and 500 nm, and the Casimir force was calculated using formulas (2) and (3) mentioned above.

As expected, the shortening of the wires of the omega particle produces a less chiral structure [21], and thus the Casimir force is minimized (see Fig. 5). Moreover, as one can notice from Fig. 5, for $a = 0.5\,\mu$m, the repulsive Casimir force becomes maximum reaching a value of 320.5 fN, while for the wires' length $0.5 \leqslant a \leqslant 1.125\,\mu$m the Casimir force almost saturates, being from 320.5 to 305.48 fN, respectively. The minor drop observed beyond $a = 1\,\mu$m is due to the increased interaction with the bottom surface, as a result of which a force pointing along the positive y axis appears.

In order to verify the effect of the sidewalls of the cavity studied in this work, a different cavity (boundary box) was designed with dimensions of $30 \times 30 \times 30\,\mu\text{m}^3$ ($E_t = 0$ along the x, y, and z directions). A single omega particle (with dimensions as described in Fig. 5) was placed inside the $30 \times 30 \times 30\,\mu\text{m}^3$ cavity at a distance of 100 nm between its upper edge and the top surface. The omega particle was displaced along the y axis (see Fig. 2) at a distance of 500 nm from the top surface of the cavity, and the Casimir force was calculated using formulas (2) and (3) mentioned above, which was practically zero ($\sim 7.7 \times 10^{-5}$ fN). Indeed, the Casimir force is six orders of magnitude less than the one calculated for the $3 \times 3 \times 3\,\mu\text{m}^3$ cavity (315.1 fN), reaching the limits of the computational method proposed within this work. This conclusion is also confirmed by the electric field distribution, which shows that less intensities are recorded (not shown here).

At this point it should be noted that the Casimir force along the x and z axes were also calculated, following the procedure described above, by moving the proposed PEC structures inside the $3 \times 3 \times 3\,\mu\text{m}^3$ cavity along the x and z directions, respectively [see Fig. 1(a)], and applying equations similar to (2) and (3). For instance, the Casimir force of the omega particle presented in Figs. 1(d) and 4 along the x axis remains repulsive, upon moving the omega particle along the x axis, from 20 to 100 nm from the right sidewall (see Fig. 4), with an intensity of $F_{x,60\text{ nm}} \sim 16.84$ fN, while the movement of the omega particle along the x axis, towards the left sidewall (see Fig. 4), provides a similar repulsive Casimir force, with an intensity of $F'_{x,60\text{ nm}} \sim 12.28$ fN. Finally, the relocation of the omega particle along the z axis, from 20 to 100 nm from the back (or front) sidewall (see Fig. 4), produces a repulsive Casimir force along the z axis, which is $F_{z,60\text{ nm}} \sim 12.14$ fN (or $F'_{z,60\text{ nm}} \sim 11.82$ fN). It is more than clear that the Casimir force of the omega particle of Fig. 1(d) embedded into the $3 \times 3 \times 3\,\mu\text{m}^3$ cavity along the x and z axes is always repulsive and almost constant to 11.82–16.84 fN, regardless of the movement of the particle along the x or z direction. Due to the symmetry of the omega particle, its movement along the z axis, either towards the front or the back sidewall (see Fig. 4), does not produce different Casimir forces: $F_{z,60\text{ nm}} \sim 12.14$ fN (or $F'_{z,60\text{ nm}} \sim 11.82$ fN). On the other hand, the omega particle is not symmetric along the y-z plane, and thus one may expect a different Casimir force when displacing the particle along the x axis towards the left or right sidewall (see Fig. 4). Indeed, when the small wire antennas of the omega particle (which induce chirality to the structure) are closer to the right sidewall, a more intense Casimir force is recorded, $F_{x,60\text{ nm}} \sim 14.84$ fN. Thus, we conclude that the Casimir f3 $\times 3 \times 3\,\mu\text{m}^3$ orce deployed between the omega particle and the metallic cavity is more sensitive and intense along the y axis than the other directions (see Fig. 4). Moreover, under the geometrical parameters remaining within the proper range of values, the Casimir force is repulsive.

In order to fully study the Casimir force of the proposed structures enclosed in the $3 \times 3 \times 3\,\mu\text{m}^3$ cavity, the medium of the cavity was assumed to be a liquid dielectric whose permittivity changed from that of vacuum to that of water [24–26]. According to several research groups [24–26], the medium in which the metal structures are embedded in plays a significant role in the nature of the reported Casimir force (attractive or repulsive). Thus, we have investigated further the PEC "omega" particle presented in Fig. 1(d), studying the effects of several media (with various ε and permeability values μ, respectively) in the $3 \times 3 \times 3\,\mu\text{m}^3$ cavity on the Casimir force between the top surface of the cavity and the structure.

As already stated, the results presented in Figs. 3 and 5 refer to PEC structures placed into the $3 \times 3 \times 3\,\mu\text{m}^3$ metallic cavities under vacuum (with $\varepsilon = 1$ and $\mu = 1$). In Fig. 6 we present the Casimir force for the omega particle presented in Fig. 1(d) embedded in the $3 \times 3 \times 3\,\mu\text{m}^3$ cavity filled with different dielectric liquids, with several ε values varying from 1 (vacuum) to 78 (water), and $\mu = 1$.

It is worth mentioning that as we increase the permittivity ε of the liquids within the cavity, from 1 to 78 (keeping the permeability μ constantly equal to 1), the Casimir force on the omega particle remains repulsive, while its intensity decreases from 315.1 fN (in the case of vacuum) to 6.14 fN (in the case of water; $\varepsilon = 78$, $\mu = 1$). As it was shown in Ref. [14], the Casimir force is directly related with the van der Waals interaction incorporating retardation effects. The latter represents the fluctuation of the electromagnetic field. It follows that the Casimir force is due to retarded interactions

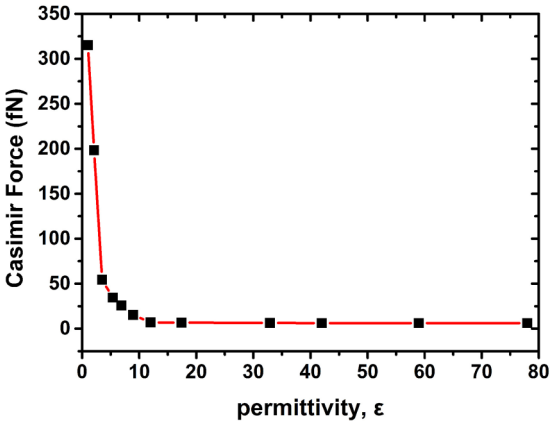

FIG. 6. (Color online) Repulsive Casimir force of the proposed "omega" particle embedded into a $3 \times 3 \times 3\ \mu m^3$ cavity, filled with various media, as a function of their permittivity ε.

between fluctuating charges developed on the walls of the cavity and those on the system. These fluctuating charges are screened very effectively by a dielectric constant intervening between the walls and the system. For two dipoles this screening is proportional to $1/\varepsilon^2$.

On the other hand, if the cavities are filled with liquids with various values of μ from 1.7 to 4.02 (and ε being constant around ∼32.7–34.82, in the case of methanol and nitrobenzene, respectively), the Casimir force is once more repulsive with an intensity of ∼8.25 fN, indicating that the permeability of the liquids in the cavity almost does not affect the Casimir force at all, in agreement with Lifshitz's theory, where all magnetic properties of the involved media are neglected with the magnetic permeability set equal to 1 [27].

IV. CONCLUSIONS AND COMMENTS

In this work we have proposed a way of calculating the Casimir force of several metallic structures embedded in a cubic cavity by taking into account the eigenmodes of the system. We have checked several designs (i.e., slabs, rings, loops, and "omega" particles) and found out that a repulsive Casimir force can be obtained by simply changing several geometrical features of the structures and mainly their distance from the sidewalls. We have also shown that the inductance and the chirality of the studied structures play a role. In addition, we have provided evidence that the medium embedded into the studied cavity (and especially its permittivity) can change the intensity of the Casimir force, while its repulsive nature, once established (owing to favorable geometrical features), remains quite robust. Finally, we want to comment on our limitation of assuming perfect metallic behavior as opposed to the realistic frequency-dependent permittivity of the metallic structures and the walls of the cavity. One can distinguish two physically distinct contributions to the Casimir force: One is due to the fluctuations of the electromagnetic field mainly in the region between the metallic surfaces, as envisioned originally by Casimir. The other is essentially a van der Waals type of interaction due to electrostatic mutual polarization of the metallic materials. It is well known [14] that the first contribution dominates at distances much larger than a characteristic absorption length $\lambda_0 \equiv c/\omega_0$ [14] and the second at distances much smaller than this length. A typical value for λ_0 is of the order of 30 nm [15]. Thus, since our calculations are for lengths considerably larger than this, we think that our conclusions are valid despite employing perfect metallic behavior.

ACKNOWLEDGMENTS

This work was supported by Greek GSRT project ERC02-EXEL, and by the European Research Council under ERC Advanced Grant No. 32081 (PHOTOMETA). Work at Ames Laboratory was partially supported by the Department of Energy (Basic Energy Sciences, Division of Materials Sciences and Engineering) under Contract No. DE-AC02-07CH11358 (computational studies).

[1] T. H. Boyer, Phys. Rev. A **9**, 68 (1974).
[2] H. B. Chan, V. A. Aksyuk, R. N. Kleiman, D. J. Bishop, and F. Capasso, Science **291**, 1941 (2001).
[3] J. N. Munday, F. Capasso, and V. A. Parsegian, Nature (London) **457**, 170 (2009).
[4] S. K. Lamoreaux, Phys. Rev. Lett. **78**, 5 (1997).
[5] F. M. Serry, D. Walliser, and J. Maclay, J. Appl. Phys. **84**, 2501 (1998).
[6] E. Buks and M. L. Roukes, Phys. Rev. B **63**, 033402 (2001).
[7] H. B. G. Casimir, Proc. K. Ned. Akad. Wet. **51**, 793 (1948).
[8] E. M. Lifshitz and L. P. Pitaevskii, *Statistical Physics: Part 2* (Pergamon, Oxford, UK, 1980).
[9] E. M. Lifshitz, Sov. Phys. JETP **2**, 73 (1956).
[10] A. Lambrecht, P. A. M. Neto, and S. Reynaud, New J. Phys. **8**, 243 (2006).
[11] S. G. Mamaev and N. N. Trunov, Theor. Math. Phys. **38**, 228 (1979).
[12] J. Ambjørn and S. Wolfram, Ann. Phys. **147**, 1 (1983).
[13] M. Bordag, U. Mohideen, and V. M. Mostepanenko, Phys. Rep. **353**, 1 (2001).
[14] A. A. Abrikosov, L. P. Gor'kov, and I. Ye. Dzyaloshinskii, *Quantum Field Theoretical Methods in Statistical Physics*, 2nd ed. (Pergamon, Oxford, UK, 1965).
[15] A. P. McCauley, R. Zhao, M. T. H. Reid, A. W. Rodriguez, J. Zhou, F. S. S. Rosa, J. D. Joannopoulos, D. A. R. Dalvit, C. M. Soukoulis, and S. G. Johnson, Phys. Rev. B **82**, 165108 (2010).
[16] T. A. Morgado, S. I. Maslovski, and M. G. Silveirinha, Opt. Express **21**, 14943 (2013).
[17] S. I. Maslovski and M. G. Silveirinha, Phys. Rev. A **82**, 022511 (2010).
[18] R. Zhao, T. Koschny, E. N. Economou, and C. M. Soukoulis, Phys. Rev. B **81**, 235126 (2010).
[19] R. Zhao, J. Zhou, T. Koschny, E. N. Economou, and C. M. Soukoulis, Phys. Rev. Lett. **103**, 103602 (2009).

[20] S. Tretyakov, A. Shivola, and L. Jylha, Photonics Nanostruct. Fundam. Appl. **3**, 107 (2005).
[21] D. L. Jaggard, A. R. Mickelson, and C. H. Papas, Appl. Phys. **18**, 211 (1979).
[22] Y. Ra'di and S. A. Tretyakov, New J. Phys. **15**, 053008 (2013).
[23] S. A. Tretyakov, F. Mariotte, C. R. Simovski, T. R. Kharina, and J.-P. Heliot, IEEE Trans. Antennas Propag. **44**, 1006 (1996).
[24] M. Bostrom, B. W. Ninham, I. Brevik, C. Persson, D. F. Parsons, and B. E. Sernelius, Appl. Phys. Lett. **100**, 253104 (2012).
[25] A. Milling, P. Mulvaney, and I. Larson, J. Colloid Interface Sci. **180**, 460 (1996).
[26] P. J. van Zwol and G. Palasantzas, Phys. Rev. A **81**, 062502 (2010).
[27] B. W. Ninham and J. Daicic, Phys. Rev. A **57**, 1870 (1998).